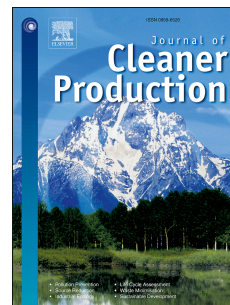


Journal Pre-proof

Energy valorization of integrating lipid extraction and hydrothermal liquefaction of lipid-extracted sewage sludge

Y. Fan, F.G. Fonseca, M. Gong, A. Hoffmann, U. Hornung, N. Dahmen



PII: S0959-6526(20)34939-8

DOI: <https://doi.org/10.1016/j.jclepro.2020.124895>

Reference: JCLP 124895

To appear in: *Journal of Cleaner Production*

Received Date: 7 July 2020

Revised Date: 30 September 2020

Accepted Date: 29 October 2020

Please cite this article as: Fan Y, Fonseca FG, Gong M, Hoffmann A, Hornung U, Dahmen N, Energy valorization of integrating lipid extraction and hydrothermal liquefaction of lipid-extracted sewage sludge, *Journal of Cleaner Production*, <https://doi.org/10.1016/j.jclepro.2020.124895>.

This is a PDF file of an article that has undergone enhancements after acceptance, such as the addition of a cover page and metadata, and formatting for readability, but it is not yet the definitive version of record. This version will undergo additional copyediting, typesetting and review before it is published in its final form, but we are providing this version to give early visibility of the article. Please note that, during the production process, errors may be discovered which could affect the content, and all legal disclaimers that apply to the journal pertain.

© 2020 Published by Elsevier Ltd.

Credit Author Statement

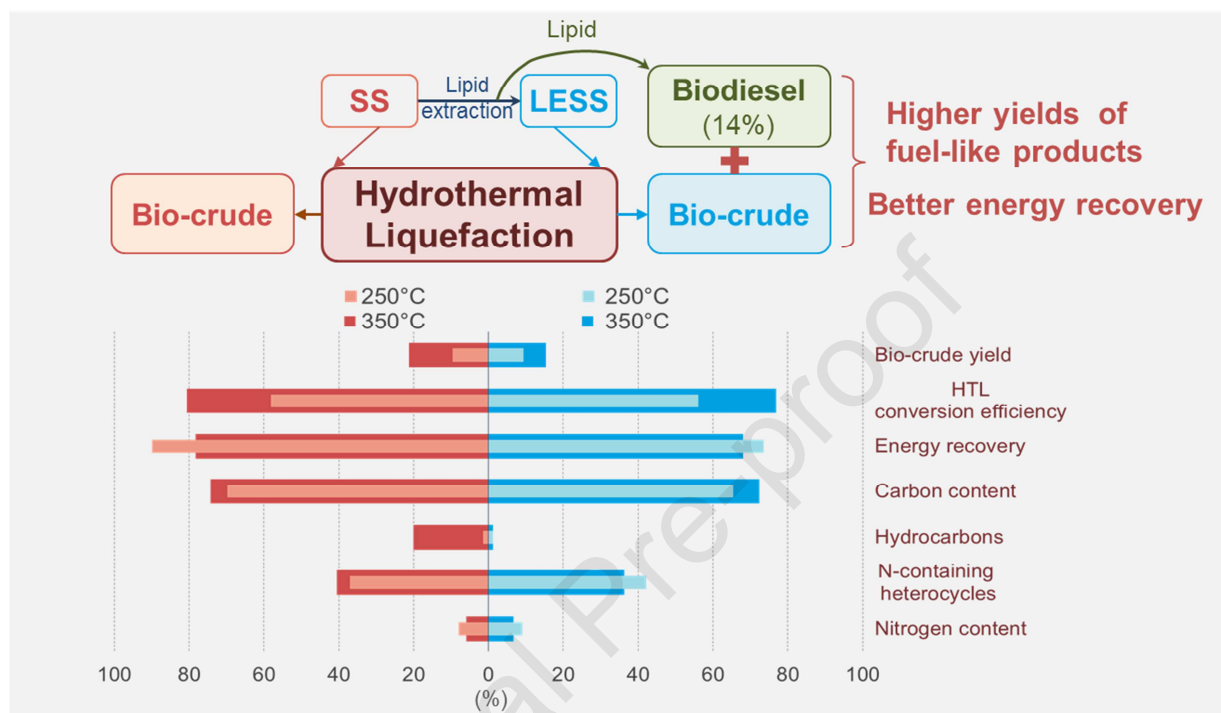
Y. Fan and A. Hoffmann designed and performed the experiments, and analyzed the data. Y. Fan and F.G. Fonseca calculated the energetic efficiency and wrote discussion. Y. Fan wrote the manuscript in consultation with M. Gong, U. Hornung and N. Dahmen. U. Hornung and N. Dahmen supervised the project, and put efforts to revise the manuscript. All authors discussed the results and commented on the manuscript.

Journal Pre-proof

Energy valorization of integrating lipid extraction and hydrothermal liquefaction of lipid-extracted sewage sludge

Journal Pre-proof

Graphical Abstract



1 **Energy valorization of integrating lipid extraction and hydrothermal liquefaction of**
2 **lipid-extracted sewage sludge**

3 *Y. Fan^{1*}, F.G. Fonseca¹, M. Gong², A. Hoffmann¹, U. Hornung^{1,3}, N. Dahmen¹*

4 ¹ *Karlsruhe Institute of Technology, Institute of Catalysis Research and Technology (IKFT),*
5 *Eggenstein-Leopoldshafen, Germany*

6 ² *Hefei University of Technology, School of Civil Engineering, Hefei, China*

7 ³ *University of Birmingham, School of Chemical Engineering, Edgbaston, Birmingham, B15*
8 *2TT, United Kingdom*

9
10 *Corresponding author.

11 E-mail address: yujie.fan@partner.kit.edu (Y. Fan)

12 **Abstract**

13 With the rapid growth in population and urbanization, a development in sustainable treatment
14 of sewage sludge has become an urgent environmental concern globally. Lipid extraction has
15 been investigated in order to valorize waste sewage sludge treatment through a pathway that
16 leads to biodiesel. In this work, an integrated approach that combines lipid extraction of
17 sewage sludge with hydrothermal liquefaction of the lipid-extracted sludge was studied in
18 order to maximize valorization. The hydrothermal process was performed at temperatures
19 ranging from 250 to 350 °C with 20 min. Regarding the bio-crude: below 300 °C, similar
20 values are found with and without lipid-extraction, with the former variant containing more
21 nitrogenated compounds stemming from Maillard reactions, while the latter more
22 hydrocarbons; at 350 °C, higher bio-crude is obtained from raw sewage sludge owing to the
23 conversion of lipids. Palmitic acid was selected as a model lipid to elucidate the role of lipids
24 during the process, as well as to provide an improved understanding of the reaction network.
25 Energy recovery reached values of 85.4 % for hydrothermal liquefaction of sewage sludge
26 and 98.3 % for integrated approach considering the whole range of biofuel products. The
27 energy consumption ratio was applied to estimate energetic efficiency for the combined
28 process, making it possible to estimate the breakeven point of the process, plus the efficiency
29 of both the hydrothermal process on its own in comparison with the combined option.

30 **Keywords:** sewage sludge; lipid extraction; HTL; biocrude; energy; Energy consumption
31 ratio

32 **1 Introduction**

33 Regarding sewage sludge (SS), a multitude of technologies has been proposed to substitute
34 traditional ways of disposal. Research has reported that landfills, composting and combustion
35 not only waste material but also create environmental problems (Cai et al., 2004; Syed-Hassan
36 et al., 2017). In addition, initiatives for the reduction of CO₂ emissions drive society to find
37 alternative sources to supply an ever-increasing demand for fuel products, providing an
38 opportunity to view sewage sludge, not as a waste, but rather as a source of carbon and energy.
39 Therefore, sewage sludge is considered a very promising waste feedstock, due to its
40 availability, as well as to its organic matter and nutrient contents (Gherghel et al., 2019;
41 Peccia and Westerhoff, 2015).

42 In order to meet the globally growing energy demand and support climate mitigation
43 strategies, the attention to make energy recovery from widespread waste has been increasingly
44 paid to disposal of sewage sludge. Biodiesel production from SS is increased in recent years,
45 because the production of biodiesel from vegetable oils has faced shortcomings associated
46 with high feedstock prices, and competition with edible crops for arable land use has limited
47 the expansion of production capacity (di Bitonto et al., 2020; Kwon et al., 2012). Sewage
48 sludge may be considered a cost-effective alternative due to its availability and lipid content,
49 typically in the range of 20 wt.% (dry ash-free basis) (Zhu et al., 2014); the lipid extraction
50 potential can reach up to 12 wt.% of the dry sludge (Supaporn and Yeom, 2016). The lipid
51 content present in sewage sludge typically consists of free fatty acids in the range of C10 to
52 C18 as precursors for the production of esters (typically methyl esters, FAME) (Siddiquee and

53 Rohani, 2011). Different methodologies can be applied for the conversion and extraction of
54 lipids from sewage sludge. Lipids may be extracted using conventional liquid-liquid methods
55 from raw sludge prior to methanolysis, or the reaction can take place directly on dry sludge or
56 dewatered sludge. Assuming an overall yield of FAMEs of 7.0 wt.% with respect to the dry
57 sludge, Dufreche et al. (Dufreche et al., 2007) reached a breakeven price of $0.83 \text{ \$}\cdot\text{L}^{-1}$, for
58 which drying the dewatered sludge (80 – 85 wt.% water) was considered the most energy and
59 cost-demanding step. Mondala et al. (Mondala et al., 2009) estimated the price of biodiesel to
60 be $0.85 \text{ \$}\cdot\text{L}^{-1}$ from in situ transesterification of dewatered sludge at an assumed yield of 10 %
61 FAMEs/dry weight of sludge. Pokoo-Atkins et al. (Pokoo-Aikins et al., 2010) reported a value
62 of $0.76 \text{ \$}\cdot\text{L}^{-1}$, by extracting lipids from the dry sludge prior to methanolysis. These values are
63 comparable to those reported for petro-diesel and show the high potential of sewage sludge as
64 a competitive lipid source for the production of biodiesel.

65 Recently, research is being focused on the performing extraction of lipids from wet sludge
66 that avoids energy-intensive drying steps. Pastore et al. (Pastore et al., 2013) carried out
67 hexane extraction directly on dewatered sludge followed by methanolysis of extracted lipids,
68 reaching to 18 wt.% FAMEs with the lowest energy demand $17 \text{ MJ}\cdot\text{kg}^{-1}$. Olkiewicz et al.
69 (Olkiewicz et al., 2014) proposed the direct sequential liquid–liquid extraction using hexane
70 for lipids is feasible and compares well with those classical pre-drying methods, 27 % (dry
71 sludge) lipids was obtained under the optimized extraction. Kech et al. (Kech et al., 2018)
72 further tested the extracting efficiency of different solvents to the direct lipid-liquid extraction
73 of lipids for biodiesel production, alternative solvents including cyclohexane/isopropyl

74 alcohol improved the yields of lipids. However, the residual sludge (lipid-extracted sewage
75 sludge, LESS) must be effectively employed to achieve favorable energy balances and
76 production costs.

77 During the last decade, hydrothermal liquefaction (HTL) is considered one of the most
78 promising technologies, as it is able to convert high-moisture feedstocks to an energy-dense
79 liquid biocrude, which could be further refined into transportation fuels. (Fox et al., 2019;
80 Kruse and Dahmen, 2018). HTL typically takes place at medium temperature ranges from
81 250 °C to 370 °C, the operating pressure is between 4 and 22 MPa, and reaction time 10 –
82 60 min (Rao et al., 2018). The yields of biocrude from sewage sludge are influenced by
83 operation parameters, type of catalysts and solvents. From previous studies of sewage sludge
84 using HTL, the biocrude produced varies from 10 to 48 wt.% (Qian et al., 2017; Suzuki et al.,
85 1988; Wang et al., 2018). Currently, some physical and chemical methods for sewage sludge
86 pre-treatment were studied. Chen et al. (Chen et al., 2020) explored the influence of
87 microwave power on yield and composition of bio-crude from HTL of SS, where increasing
88 the microwave power can improve the biocrude yields by between 2 – 10 %. Kapusta
89 (Kapusta, 2018) reported that the ultrasound pretreatment can achieve 19 % increase
90 bio-crude from HTL of SS 320 °C compared with un-treated sludge. Co-liquefaction SS with
91 other types of feedstocks has attracted considerable research interest as it aims to increase
92 biocrude yield with improving quality (Yang et al., 2019). Fox et al. (Fox et al., 2019)
93 conducted the hydrothermal co-liquefaction of food waste and SS after 200 °C pretreatment.
94 To the best of our knowledge, limited information is available considering the integration of

95 HTL and lipid extraction. Based on the success in using LESS as anaerobic digestion
96 feedstock (Olkiewicz et al., 2014), and the proven feasibility of using lipid-extracted algae
97 residue (Frank et al., 2012; Shahi et al., 2020; Vardon et al., 2012) and de-oiled yeast (Chopra
98 et al., 2019) in HTL, the integration of both these processes is attractive due to the maximum
99 utilization of sewage sludge, as well as the different products obtainable. When disregarding
100 the water content, LESS is mostly comprised of proteins and carbohydrates. In particular,
101 proteins have been confirmed to promote to bio-crude production using HTL (Posmanik et al.,
102 2017). Maillard reactions play a significant role in the bio-crude product distribution and
103 composition, which is caused by the reaction of amine groups present in proteins with
104 carbonyl groups present in reducing carbohydrates (Fan et al., 2018; Zhang et al., 2016).

105 Therefore, the objectives of this paper are: 1) to quantify and characterize the extracted lipids
106 from sewage sludge and to evaluate their applicability for biodiesel production; 2) to
107 investigate the hydrothermal conversion efficiency of LESS through HTL, comparing the
108 different products generated by HTL of SS and LESS in order to evaluate whether LESS can
109 be a potential feedstock for the production of fuel components; 3) to reveal the effect of lipids
110 on bio-crude products based on model compounds with an improved understanding to
111 reaction pathways; 4) to estimate the coupling effect of lipids extraction and HTL of LESS, in
112 terms of the yields of fuel-like products and process efficiency.

113 **2 Materials & methods**

114 **2.1 Materials**

115 Digested sewage sludge (SS) was obtained from a wastewater treatment plant (WWTP) in
116 Plieningen, Stuttgart, Germany. The SS sample was collected from the WWTP and stored at
117 -18 °C until use. The sludge was used directly as received (moisture content 78.75 wt.%) in
118 this work. Crude protein was determined by Kjeldahl method, carbohydrates was determined
119 by using the phenol-sulfuric acid photometric estimation by DuBois method (Jimenez et al.,
120 2013).

121 Methanol, sodium bicarbonate, sodium chloride, and palmitic acid (PA) were supplied by
122 Sigma-Aldrich, analytical grade. Supelco 37 Component FAME Mix used as a standard
123 solution was purchased from Restek. The same supplier provided HPLC grade
124 dichloromethane (DCM), tetrahydrofuran, and hexane.

125 **2.2 Lipid extraction and quantification**

126 Extraction was carried out in a Soxhlet apparatus using hexane mixed with ethanol as a
127 solvent (1:1 vol.%) (Zhu et al., 2014). For practical operation, 5 g of dried sample were
128 poured in the thimble and 90 mL solvent mixture was placed in the still pot. Extraction was
129 performed at a temperature that ranged from 70 to 80 °C and sustained for about 6 h. After
130 extraction, the mixed solvent was removed using a rotary evaporator at 40 °C under vacuum
131 at 50 mbar. Then, the remnant lipid fraction was stored in a desiccator overnight and weighed
132 the next day to determine the extraction yield. The left residual was air-dried and defined as
133 lipid-extracted sewage sludge (LESS).

134 In-situ transesterification of sewage sludge was conducted by reactive extraction by adapting
135 the method presented by Mondala et al. (Mondala et al., 2009), which goes as follows: 2 g of
136 freeze-dried sludge was weighed into a 250 ml flask. The sludge samples were then treated at
137 75 °C, 5 ml (5 vol.%) H₂SO₄, and 24 ml methanol (mass ratio of methanol to dried sludge
138 (12:1)). 25 ml of hexane was added to improve the lipid solubility in the reaction mixture. The
139 sludge was then suspended in a solution using a magnetic stirring bar and the mixture was
140 heated to the set temperature using a hot water bath with a retention time of 8 h. After the
141 reaction was stopped, the mixture was allowed to cool, and the flask contents were transferred
142 into a 100 ml bottle. Then, 2.5 ml of saturated NaCl solution and 25 ml of hexane were added.
143 The mixture was then centrifuged at 3000 rpm for three minutes and the supernatant hexane
144 phase was withdrawn and transferred into a 100 ml round-bottom flask. The extraction
145 procedure was repeated three times. Afterward, the total volume of the collected supernatant
146 was washed with 5 ml of a 2 % (w/v) sodium bicarbonate solution and the aqueous phase was
147 allowed to settle. The upper layer passed through a filter paper containing anhydrous sodium
148 sulfate before being collected.

149 FAME content in the hexane phase was analyzed using a Shimadzu GC-FID (Agilent 7890 B).
150 A Stabilwax-DA, 30 m × 0.25 mm × 0.25 mm column was used for the analysis. The column
151 temperature was programmed to start at 40 °C, to be maintained for 10 min, and then to be
152 increased from 40 to 250 °C for 10 min at 8 °C/min. The sample injection volume was 1.0 µl,
153 with a split ratio of 10:1. Injection of standard solutions (Supelco 37 Component FAME Mix)
154 with distinct concentrations and examination of the linear regression of the responses aided

155 determination of the linearity. For example, the linear correlation coefficients were 0.99857
156 for palmitic acid (C16:0) ($y = 0.87773489x - 14.148712$) and 0.99876 for stearic acid (C18:0)
157 ($y = 0.88245915x - 8.9711545$). Construction of the analytical curves enabled us to describe
158 the mathematical equations used for quantitation and calculations.

159 **2.3 Hydrothermal liquefaction**

160 Each sample was liquefied in micro-autoclaves with a volume of 24.5 ml made of stainless
161 steel (1.4571 Ti), which can withstand pressures of up to 40 MPa and a maximum temperature
162 of 400 °C. The reactors were loaded with sludge slurry, 25 wt.% (dry-free basis). It should be
163 noted that the lipid-extracted sludge was mixed with water to achieve similar conditions to
164 dewatered sludge. For the case of palmitic acid, each batch consisted of 10 wt.%. The
165 micro-autoclaves were flushed to remove the undesired air and then pressurized to 2 MPa
166 using nitrogen gas. Heating was performed in a gas chromatography (GC) furnace at a heating
167 rate of 40 K/min and kept at the target temperature (250, 300, or 350 °C) for 20 min. After the
168 reaction, the autoclaves were taken out of the oven and put in cold water to cool down and to
169 stop the reaction. All the experiments were executed in triplicates to assess standard deviation
170 (error bars in figures).

171 *Product separation and analysis*

172 After the HTL reaction, the micro-autoclaves were opened in a gas-tight containment after
173 flushing air out using nitrogen. The gas composition was measured by manually injecting
174 100 µl of the gas sample in an Agilent 7890A gas chromatograph (equipped with a 2 m
175 Molsieve 5 Å and 2 m Porapak Q column). The mixed products including aqueous phase,

176 bio-crude and solid residue were washed with dichloromethane (DCM) and filtered through
177 vacuum filtration using a Whatman nylon membrane (47 mm, 0.45 μm pore size). Most of the
178 bio-crude remained stuck to the micro-autoclave walls after the reaction, so additional use of
179 DCM was required to maximize the recovery of products. The solid residue remaining in the
180 filter was placed in an oven and dried overnight at 105 $^{\circ}\text{C}$ to determine the dry weight. The
181 biphasic mixture obtained (aqueous product plus bio-crude) was centrifuged and separated.
182 The organic solvent was evaporated by flushing with nitrogen for 24 h. Once a constant
183 weight had been achieved, it was recorded and considered as the bio-crude mass.

184 The C, H, and N contents of the bio-crude and the solid residue were measured using a Vario
185 EL III analysis system (Elementar Analysensysteme GmbH, Hanau, Germany). Oxygen
186 content was calculated by difference.

187 GC-MS analysis of bio-crude was carried out using an Agilent 6890N gas chromatograph
188 with an Agilent 5973 MSD mass spectrometry detector and a DB-5 capillary column ($30 \times$
189 $0.25 \text{ mm} \times 0.25 \mu\text{m}$) after diluting with tetrahydrofuran (1:1 ml/ml) and filtering with a
190 $0.20 \mu\text{m}$ polytetrafluoroethylene (PTFE) Filter. The substances were identified using the NIST
191 library, considering only molecules with a match quality above 80 %. The amount of the
192 different compounds was estimated by the relative area percentage method.

193 Thermal gravimetric analysis (TGA, Mettler toledo DSC 822) approximately 10 mg of the
194 samples was measured within the range from 20 to 800 $^{\circ}\text{C}$ with a heating rate of 10 K/min
195 and N_2 flow rate of 50 ml/min, to apply a method devised by Liu et al. (Liu et al., 2018) for
196 the assessment of the fractionation potential of produced bio-crude in a petroleum refinery

197 environment. The total carbon (TC), total organic carbon (TOC), total inorganic carbon (TIC),
 198 and total nitrogen (TN) in the aqueous phase were measured with a Dimatec® 2100
 199 instrument. Ammonium (NH_4^+), nitrate (NO_3^-), and nitrite (NO_2^-) were investigated by
 200 Metrohm 838 advanced sample processor device. Organic acids were analyzed with an
 201 Aminex HPX-87H column (Biorad, Hercules, CA, USA).

202 **2.4 Data definition**

203 The yields (Y_i) of the different product fractions were calculated as the weight of the
 204 recovered mass of organic matter in the product (OM_i) related to the total mass of organic
 205 matter in the feedstock ($OM_{\text{feed, daf.}}$), see Eq. (1).

$$206 \text{ Product Yields (wt. \%)} = \frac{OM_i}{OM_{\text{feed}}} \times 100 \quad (1)$$

207 The HTL conversion efficiency was calculated as the difference in feedstock mass (OM_{feed})
 208 and solid residue (OM_{SR}) (assuming this to be unconverted feedstock) related to the feedstock
 mass (OM_{feed}), as shown in Eq. (2).

$$209 \text{ HTL conversion efficiency (\%)} = \frac{OM_{\text{feed}} - OM_{\text{SR}}}{OM_{\text{feed}}} \times 100 \quad (2)$$

210 The elemental distribution, namely carbon distribution (CD) and nitrogen distribution (ND)
 211 are defined as the amount of an element in the product (m_{Ei}) relative to the amount in the
 feedstock product ($m_{E\text{feed}}$), see Eq. (3).

$$212 \text{ Elemental Distribution (wt. \%)} = \frac{m_{Ei}}{m_{E\text{feed}}} \times 100 \quad (3)$$

213 Higher heating value (HHV; $\text{MJ}\cdot\text{kg}^{-1}$) was estimated using the modified Dulong's formula
 (Posmanik et al., 2017) as given in Eq. (4).

$$\text{HHV (MJ/kg)} = 0.0338 \times C + 1.428(H - O/8) \quad (4)$$

214 The energy recovery (ER) as the sum of the higher heating values (HHV_i) of the recovered
 215 fuel-like products (bio-crude, bio-char, when necessary, extracted lipids) weighed by their
 216 yield Y_i^* relative to the value (HHV_{feed}) of the dry feedstock, see Eq. (5).

$$ER (\%) = \frac{\sum (Y_i^* \times HHV_i)}{HHV_{feed}} \times 100 \quad (5)$$

217 The concept of ECR (Energy Consumption Ratio, Eq. (6)), was employed by Sawayama et
 218 al. (Sawayama et al., 1999) and Minowa et al. (Minowa et al., 1998) to estimate the energetic
 219 viability of the process by relating the heat demands of the process to the heating value of the
 220 products. Values lower than 1 indicate a good energetic balance, revealing that the energy
 221 content of the products (E_0) is higher than the energy requirement of the production process
 222 (E_L).

$$ECR = \frac{E_L}{E_0} \quad (6)$$

223 For the case of hydrothermal liquefaction, the authors propose the following formula (Eq. (7)),
 224 for which w_i is the water content, $c_{p,w}$ is the specific heat of liquid water ($4.18 \text{ kJ}\cdot\text{kg}^{-1}\cdot\text{K}^{-1}$), $c_{p,s}$
 225 is the specific heat of dry solid ($1.25 \text{ kJ}\cdot\text{kg}^{-1}\cdot\text{K}^{-1}$), ΔT is the temperature difference to ambient
 226 temperature ($25 \text{ }^\circ\text{C}$), Y_i is the product yield (wt.% daf.), and w_0 is the organic fraction of the
 227 feedstock sludge (wt.% daf.).

$$ECR_{HTL} = \frac{E_L}{E_0} = \frac{[w_i c_{pw} \Delta T + (1 - w_i) c_{ps} \Delta T](1 - r_2)}{[(1 - w_i) Y_i (HHV) w_0] r_1} \quad (7)$$

228 For the complete process chain, the concept of ECR was extended to additional process steps
 229 (Eq. (8)), which make use of heat demands (Q_i) and product energy potentials (E_i). Four
 230 different process configurations were considered: 1) HTL to produce only bio-crude (ECR_{BC}),
 231 which employs Q_{HTL} and E_{BC} ; 2) HTL to produce bio-crude and solid residue as energy

232 carriers (ECR_{BC+SR}), which employs Q_{HTL} , E_{BC} , and E_{SR} ; 3) considering HTL products and
 233 lipid extraction ($ECR_{BC+SR+L}$), which employs Q_{HTL} , Q_{drying} , $Q_{extraction}$, E_{BC} , E_{SR} , and E_{LIPID} ; 4)
 234 considering HTL products and FAME production from the lipids extracted ($ECR_{BC+SR+FAME}$),
 235 which employs Q_{HTL} , Q_{drying} , $Q_{extraction}$, $Q_{methanolysis}$, E_{BC} , E_{SR} , and E_{FAME} .

$$ECR = \frac{E_L}{E_O} = \frac{(\sum Q_{step})(1 - r_2)}{(\sum E_{product})r_1} \quad (8)$$

236 The efficiency of combustion (r_1) and the efficiency of heat recovery (r_2) can be adjusted
 237 depending on the technology employed. Sawayama et al. (Sawayama et al., 1999), in 1999,
 238 used values for r_1 and r_2 of 0.6 and 0.5, respectively. On the other hand, more up-to-date
 239 values of 0.7 and 0.5 have been proposed by Vardon et al. (Vardon et al., 2012) and an
 240 optimized hypothetical case using state-of-the-art combustion and heat recovery technology
 241 may permit reaching values of 0.9 and 0.6 (Demirbas, 2009). The latter two situations are
 242 considered during the discussion of results, and are named the case A and case B, respectively.
 243 As per Eq. (9) (Sawayama et al., 1999), Q_{HTL} , the heating demand of the hydrothermal
 244 liquefaction process was estimated as the sensible heat required to increase the temperature
 245 (ΔT) of the mixture (water + dry sludge) to the target temperature. No phase change was
 246 assumed to take part during the HTL process.

$$Q_{HTL} = w_i c_{pw} \Delta T + (1 - w_i) c_{ps} \Delta T \quad (9)$$

247 For the case of drying (Eq. (10)), a final temperature of 100 °C was assumed with $\Delta H_{vap,w}$ as
 248 the heat of vaporization of water (2.26 MJ·kg⁻¹) and HHV_s as the higher heating value of the
 249 sludge.

$$Q_{drying} = [w_i (\Delta H_{vap,w} + c_{pw} \Delta T) + (1 - w) c_{ps} \Delta T] \quad (10)$$

250 $Q_{extraction}$ was assumed to be $60.95 \text{ MJ}\cdot\text{kg}^{-1}_{\text{lipid}}$ taken from Olkiewicz et al.(Olkiewicz et al.,
 251 2012), and a value of 934 Btu/lb ($2.17 \text{ MJ}\cdot\text{kg}^{-1}$) was obtained for the demand of the
 252 methanolysis process ($Q_{methanolysis}$) given by Huo et al. (Huo et al., 2009). A value of
 253 $39.5 \text{ MJ}\cdot\text{kg}^{-1}$ was assumed as the heat of combustion of FAME (Pastore et al., 2013).
 254 The specific energy demand (ED, Eq. (11)) serves as another indicator of the energetic
 255 efficiency of the process, in such a way that it can be compared to other values reported in the
 256 literature or to other processes. It was calculated using both FAME and bio-crude as mass
 257 basis, due to being the products of main interest.

$$ED\left(\frac{\text{MJ}}{\text{kg}_{\text{product}}}\right) = \frac{(\sum Q_{\text{step}})(1 - r_2)}{m_{\text{product}}} \quad (11)$$

258 3 Results

259 3.1 Feedstock composition

260 The properties of sewage sludge (SS) and lipid-extracted sludge (LESS) are outlined in Table
 261 1. Protein was found to be the predominant fraction, accounting for 34.6 wt. % and 38.9 wt.%
 262 in sewage sludge and lipid-extracted sludge respectively. which lays within the range
 263 available in the literature (30 – 60 wt.%) (Gao et al., 2020), including raw primary sludge ,
 264 secondary sludge , and digested sludge . The results were quite consistent after 5 runs with 10
 265 parallel repetitions each. Lipids were found to be a minor component of sludge, constituting
 266 13.9 wt.% of the raw material.

Table 1. Characterization of sewage sludge and lipid-extracted sludge.

feedstock	Biochemicals (wt.% daf) ^a				Ash	Elemental content (wt.%) ^b					HHV (MJ·kg ⁻¹)
	carbohydrates	proteins	lipids	others		C	H	O ^c	N	S	
SS	27.9	34.6	13.9	23.6	38.6	25.8	4.6	26.6	3.7	0.7	10.5
LESS	31.3	38.9	-	29.8	45.3	24.0	4.1	22.2	3.8	0.6	10.0

^a: on the ash-free basis

^b: on the dry basis

^c: calculated by difference to the total mass

267 Elemental analysis was also displayed in Table 1. Special care must be given to the nitrogen
 268 content in the feedstock, as this is an important control parameter for the quality of bio-crude ,
 269 due to the formation of NO_x during combustion and demanding treatment during bio-crude
 270 upgrading. However, protein-rich sludge may still be desirable because of the higher
 271 thermochemical bio-crude conversion efficiencies compared to those obtained with biomass
 272 that is richer in more recalcitrant carbohydrates and lignin (Vardon et al., 2012). Raw sludge
 273 showed a slightly higher energy content due to its lipids content.

274 Regarding lipid extraction, many methods with different procedures can be found in
 275 publications, of which a summary is provided in Table 2 below. Generally, Soxhlet extraction
 276 is quite effective in extracting lipids from both dry and wet sludge (Zhu et al., 2014) (Inoue et
 277 al., 1996) (Olkiewicz et al., 2014) (Boocock et al., 1992). It was assumed that all lipids
 278 present in the original material were extracted. The organic material was analyzed for
 279 carbohydrate, protein and lipid content, others may include lignin and fiber content.

Table 2. Summary of lipid extraction from published sources.

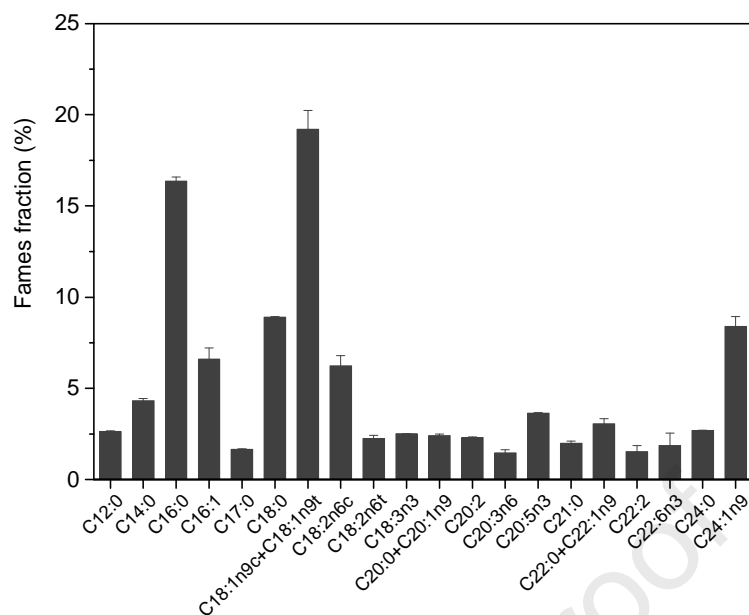
Feedstocks	Fractions	Content wt.%(db)	Methods (solvent)	Reference
Primary mixed waste activated sludge	Crude fat	10.4	-	(Dote et al., 1992)
Digested sludge raw primary sludge waste active sludge	Crude fat	1.9-12.2	ether solvent	(Suzuki et al., 1988)
Secondary SS	Lipid	8.01		(Wang et al., 2018)
Dewatered SS	Lipid	5.0	Soxhlet extraction	(Inoue et al., 1996)
Liquidized SS	Lipid	10.4	(Diethyl ether)	

Digested sludge	Crude-lipid	<1	Ether solvent	(Vardon et al., 2011)
Dewatered sludge	Lipid	2.5-10.3	Soxhlet extraction (hexane-ethanol)	(Zhu et al., 2014)
		2.2-7.5	Acid hydrolysis	
		3.0-7.5	Water bath shaking	
Primary SS			Soxhlet extraction (hexane)	(Olkiewicz et al., 2014)
Secondary SS	Lipid	7.7-26.2	Liquid-liquid	
Blended sludge			Extraction (hexane)	
Raw sewage sludge	Lipid	12	Soxhlet extraction (chloroform)	(Boocock et al., 1992)
		17-18	Boiling extraction (chloroform)	

-: Not mentioned

280 3.2 Lipid extraction from sewage sludge

281 The fatty acid composition of the lipids from the SS was inferred from the results of the
 282 FAMEs produced by the *in-situ* transesterification of dry sludge samples. In Figure 1, it can
 283 be clearly seen that a significant amount of methyl esters belong to relatively short chains
 284 below C18, the cumulative amount of C16:0 and C18:1 was more than 70 %, which was
 285 similar to the value in another report (Olkiewicz et al., 2014). The results show a
 286 predominance of palmitic acid (C16:0), stearic acid (C18:0), oleic acid (C18:1), in line with
 287 previous work. Specifically, palmitic acid was the major saturated fatty acid with a value of
 288 16.4 %, followed by stearic acid accounting for 8.9 %. Oleic acid was the major unsaturated
 289 fatty acid, followed by docosahexaenoic acid (C24:1). These fatty acids are exceptionally
 290 well-suited for the production of biodiesel (Olkiewicz et al., 2012; Siddiquee and Rohani,
 291 2011; Zhu et al., 2014).



292

293 Figure 1. FAMES analysis of biodiesel obtained from the in-situ transesterification of SS.

294 3.3 HTL of residue from lipid-extracted sewage sludge (LESS)

295 In this chapter, raw sewage sludge is used as “reference” to compare the hydrothermal
 296 conversion and the products obtained from the HTL of SS and LESS.

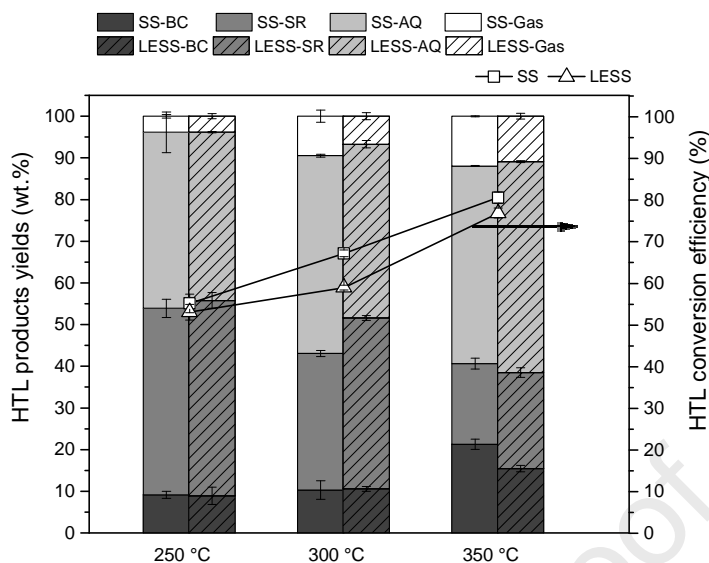
297 3.3.1 HTL conversion

298 A general comparison between the HTL of SS and LESS is shown in Figure 2, where BC, SR
 299 and AQ represent the bio-crude, solid residue and aqueous phases, respectively. Both HTL
 300 conversion efficiency (see Eq. (2)) and bio-crude yield increase with the temperature for either
 301 feedstock, although HTL of SS shows higher conversions than HTL of LESS for the same
 302 operating conditions. Compared to results (average 25 wt.%) reported by other studies using
 303 similar operating conditions, the bio-crude yields reported in this manuscript are lower (Liu et
 304 al., 2018; Suzuki et al., 1988). At 250 °C and 300 °C, the yields of biocrude obtained from
 305 HTL of SS and LESS are basically the same; however, a difference occurs at 350 °C, where

306 the bio-crude yields reach values of 21.3 and 15.4 wt.% for SS and LESS, respectively. In
307 contrast, the SR decreases with the reaction temperature. Compared to HTL of LESS, HTL of
308 SS results in lower solid residue yields at the temperatures used. The AQ forms the dominant
309 part of all the products, between 36.6 to 50.6 wt.% in all cases, and slightly increased with
310 reaction temperature.

311 **3.3.2 Carbon and nitrogen balance**

312 Table 3 shows the elemental balance/distribution in different phases, namely, carbon
313 distribution (CD) and nitrogen distribution (ND), estimated using Eq. (3). For both SS and
314 LESS, the carbon content in the SR significantly decreases from 64.1 to 29.1 % and 58.2 to
315 38.5 % with a temperature increase from 250 to 350 °C, respectively. In the bio-crude phase,
316 the CD correspondingly increases from 13.5 to 34.0 % and from 12.5 to 27.6 %, respectively.
317 The CD of the AQ seems stable, only showing a slight trend of decreasing with the reaction
318 temperature. When considering the gas formed, while the yields are low (< 12 wt.%), the CD
319 shows a rise by a factor of around 4 from 250 to 350 °C.



320
 321 Figure 2. Comparison between HTL of SS and LESS at different temperatures, the yield of the
 322 aqueous phase (AQ) was determined as the difference between unity and the sum of the yields
 323 of bio-crude (BC), solid residue (SR), and bio-gas (Gas) fractions.

324 Nitrogen has also been investigated as another important element with regard to the high
 325 protein content in both SS and LESS. In contrast to what was discussed for the case of carbon,
 326 nearly half the amount of nitrogen is recovered in the aqueous phase under all conditions. Due
 327 to this high nitrogen content, the aqueous phase has been considered as a promising medium
 328 to cultivate algae, with some success (Biller et al., 2012; Jena et al., 2011). With increasing
 329 temperature, the ND in the SR of SS and LESS is significantly reduced from 37.5 to 21.1 %
 330 and 35.7 to 22.1 %, respectively. For the case of bio-crude, increasing reaction temperatures
 331 seem to lead to increased incorporation of nitrogen, as ND increases from 10.3 to 20.8 % as
 332 the temperature rises from 250 to 350 °C, affecting the usability of this phase.

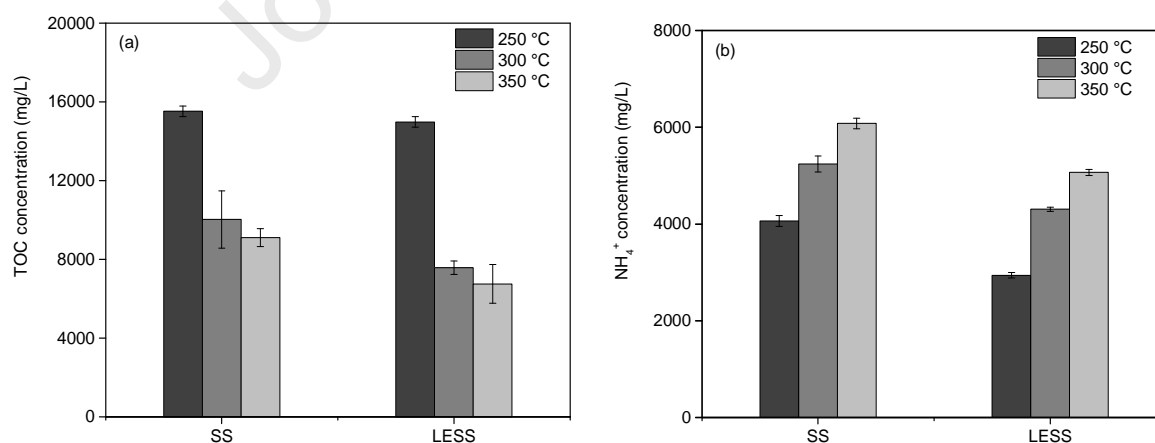
333 HTL resulted in a considerable proportion of dissolved organic carbon and a major proportion
 334 of N in its aqueous phase in every case. Total organic carbon (TOC) analysis was applied to
 335 determine water-soluble organic products, as shown in Figure 3 (a). After HTL of SS and of

336 LESS, TOC contents significantly decreased as the temperature increased from 15500 to
 337 9000 mg/L and 14900 to 6700 mg/L, respectively. While at 250 °C, the TOC in the aqueous
 338 phase from SS and LESS are similar, at higher temperatures, the TOC observed for the
 339 aqueous phase from LESS were lower than that from SS.

Table 3. Carbon/Nitrogen distribution (CD/ND, wt.%) of various products.

Samples	Bio-crude		Solid		Aqueous phase		Gas	Recovery	
	CD	ND	CD	ND	CD	ND	CD	CD	ND
SS-250 °C	13.5	10.3	64.1	45.5	19.6	48.8	2.5	99.8	104.6
SS-300 °C	17.1	12.1	53.6	38.0	15.6	47.1	6.2	92.6	97.2
SS-350 °C	34.0	20.8	29.1	25.6	14.8	42.2	8.2	86.2	88.7
LESS-250 °C	12.5	11.0	54.6	40.2	21.3	42.2	2.2	90.7	93.4
LESS-300 °C	17.3	11.5	49.2	35.9	15.6	45.2	4.6	86.7	92.6
LESS-350 °C	27.6	16.7	38.5	31.3	14.0	44.6	9.4	89.6	92.5

340 Regarding ammonium (NH_4^+), seen in Figure 3 (b), the opposite trend was observed. After
 341 HTL of SS and LESS, NH_4^+ concentrations steadily increased with the temperature from 4000
 342 to 6000 mg/L and 3000 to 5000 mg/L, respectively. In addition, the NH_4^+ content present in
 343 the AQ phase after HTL of SS was higher than that of LESS under the same conditions.



344
 345 Figure 3. Total organic carbon concentration (a) and ammonium concentration (b) in the
 346 aqueous phase from HTL of SS and LESS

347 3.3.3 Energy content of the products

348 Table 4 summarizes element ratios and HHV for all bio-crude and solid products. Further

349 detailed elemental analyses are shown in Table S1. The extracted lipids exhibit HHV very
 350 similar to that of FAME (39.29 vs 39.5 MJ·kg⁻¹) (Pastore et al., 2013).

351 When comparing the raw SS and LESS, the bio-crude obtained from HTL shows a lowering in
 352 the H/C and O/C ratios and higher HHV. The effect of temperature is most noticeable when
 353 comparing the results at 250 °C and 300 °C, but the change between 300 °C and 350 °C is
 354 subtle and may lay within experimental uncertainty; this trend can be observed for
 355 experiments using both SS and LESS. Regarding the solid residue, HTL treatment led to
 356 lower H/C and O/C ratios when compared to the feedstocks. The effect of temperature seems
 357 to be similar to that found for bio-crude. All heating values ranged from 28 to 40 MJ·kg⁻¹,
 358 close to those reported for bio-crude produced from sewage sludge (35 – 40 MJ·kg⁻¹) (Qian et
 359 al., 2017) and paper sludge (35 – 37 MJ·kg⁻¹) (Xu and Lancaster, 2008), but lower than that of
 360 petroleum crude oil (43 MJ·kg⁻¹) (Speight, 2015). Low N/C ratios in the bio-crude and high
 361 values in the solid residue confirm the results presented in Table 3.

Table 4. Elemental composition (atomic ratio), higher heating value (MJ·kg⁻¹) of bio-crude and solid residue.

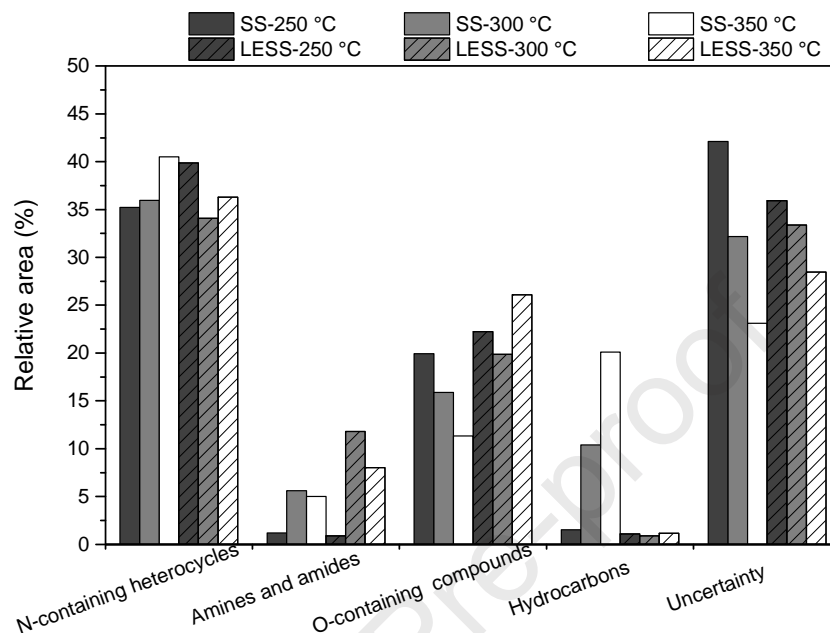
HTL	Bio-crude				Solid residue			
	H/C	O/C	N/C	HHV	H/C	O/C	N/C	HHV
Raw SS					0.77	2.14	0.12	10.54
LESS					0.70	2.07	0.13	10.03
Extracted lipids	1.86	0.11	0.01	39.29				
SS-250 °C	0.18	1.62	0.09	32.29	0.38	1.56	0.09	10.02
SS-300 °C	0.13	1.57	0.09	34.60	0.16	1.41	0.09	10.35
SS-350 °C	0.09	1.57	0.07	37.26	0.22	1.39	0.11	6.40
LESS-250 °C	0.24	1.56	0.12	28.85	0.48	1.52	0.10	8.29
LESS-300 °C	0.11	1.45	0.09	34.76	0.49	1.31	0.10	7.11
LESS-350 °C	0.12	1.45	0.08	34.91	0.27	1.33	0.11	6.82

362 3.3.4 Bio-crude composition

363 Figure 4 shows the groups of chemicals in the bio-crudes obtained. The identification of
364 organic compounds was achieved by comparing the spectra of sample components (limited to
365 the top 50 compounds based on the peak-normalized volume) with those in the electronic
366 library of NIST. The organic components were analyzed using the area normalization
367 method (Li et al., 2014). Detailed categories of constituents can be seen in Table S2 in the
368 Supporting Information. The identified components account for more than 56 % and 64 % of
369 the total species in the bio-crude derived from SS and LESS, respectively. The major detected
370 compounds are N-containing heterocycles such as pyrazines, pyrrolidinones, and indoles,
371 similar species have been described in a previous report (Zhai et al., 2014). These fractions
372 slightly increase with reaction temperature in the case of HTL of SS. A decrease is observed
373 from HTL of LESS. O-containing compounds form the second largest constituent of bio-crude,
374 mainly composed of phenolic compounds. It is observed that O-containing compounds in the
375 bio-crude from HTL of SS greatly decrease with increasing temperature, whereas, conversely,
376 a higher amount of O-containing compounds are formed in the case of HTL of LESS. The
377 yield of hydrocarbons seems to be very influenced by the temperature (an increase from 1.5 to
378 20.1 %) for the case of SS, but an almost absence of these compounds in bio-crude produced
379 from LESS, due to negligible lipid content.

380 Regarding amines and amides, the lowest fractions are produced at 250 °C which may be a
381 temperature too low to promote this type of reaction. Bio-crude from LESS shows a higher
382 value of said components, mostly including piperidines and acetamides. While, around 1.5 %

383 hexadecanamide could be found in bio-crude stemming from HTL of SS at 300 °C, indicating
 384 reactions between lipid and protein contents.



385
 386 Figure 4. Chemical groups represented in bio-crude obtained from HTL of SS and LESS under
 387 different temperatures.

388 TGA analysis was applied to study the three stages of weight loss and its relationship to the
 389 results of GC-MS analyses of the composition of the bio-crude. The TGA curves of the 6
 390 kinds of bio-crude from HTL of SS and LESS are shown in Fig. S1 in the Supporting
 391 Information. All HTL bio-crudes show the same TGA curve progression, with a similar
 392 decomposition process. However, the derivative thermogravimetry (DTG) plot seems to be
 393 quite different. The DTG curves of bio-crude from HTL of SS at 300 and 350 °C show weight
 394 loss at 100 °C, indicating the presence of water. A relatively significant weight loss takes
 395 place between 180 °C and 380 °C with a peak at 290 °C. Regarding the HTL of LESS, a
 396 relatively significant weight loss occurs between 150 °C and 330 °C with no specific peak.
 397 Another significant decomposition process is triggered at around 430 °C.

398 Table 5 further provides boiling point distributions which were calculated based on the weight
 399 loss during TGA measurement. Small differences in boiling point distribution trends are
 400 observed for HTL bio-oils derived from SS and LESS. The most significant fractions
 401 correspond to compounds of volatilities similar to those of kerosene or diesel oil (200 °C to
 402 400 °C), in agreement with results found by Liu et al. (Liu et al., 2018). LESS bio-crude
 403 contains more fractions in the gasoline range (110 – 200 °C) and less in the heavy diesel (300
 404 – 400 °C) when compared to SS bio-crude. The amount of distilled fractions between 200 °C
 405 and 550 °C, which can generally be used in petroleum refineries (Huang et al., 2016),
 406 accounted for around 71 to 74.1 wt.% in bio-crude from HTL of SS, and 67.2 to 70.9 wt.% in
 407 bio-crude from HTL of LESS. Accordingly, it is worth noting that the heavy crude fraction
 408 (> 550 °C) in all bio-crude is larger than 25.9 wt.%, the value reported from Liu et al. (Liu et
 409 al., 2018), limiting the chances of direct refinery integration and requiring costly upgrading.
 410 More residues at higher boiling points (> 800 °C) were obtained in the crude derived from
 411 HTL of LESS.

Table 5. Boiling point distribution of bio-crude from HTL of SS and LESS.

Distillation Range (°C)	typical application ^a	Distribution (wt.%) in Bio-crude					
		SS			LESS		
		250 °C	300°C	350 °C	250 °C	300 °C	350°C
20-110	Bottle gas	3.3	2.6	2.8	2.3	3.8	1.6
110-200	Gasoline	12.7	11.8	13	14.7	19.7	14.7
200-300	Jet fuel/Light diesel	24.9	22.9	23.8	23.2	21.3	24.0
300-400	Heavy diesel	22	20.4	14.4	13.2	12.3	12.6
400-550	Vacuum Gas Oil	11.2	15.6	17	15.2	13.8	14.3
<550		74.1	73.3	71	68.5	70.9	67.2
550-700	Heavy Fuel Oil	3.9	2.8	5.1	3.7	6.9	4
700-800	Asphalt	1.7	1.3	3.1	2.4	5.2	2.0

>800	Residue	20.3	22.6	20.8	25.4	17	26.8
------	---------	------	------	------	------	----	------

^a: Handbook of Petroleum Product Analysis (Speight, 2015)

412 **4 Discussion**

413 **4.1 Possible reaction pathways for HTL of LESS**

414 Figure 2 shows that the conversion of SS and LESS via HTL is comparable, suggesting that
415 the residue after lipid extraction can be considered a suitable feedstock for the HTL process.

416 For both cases, increasing temperature leads to increased conversion, along with a decrease of
417 organic content in the solid residue. A lower amount of solid residue overall is found when
418 using raw SS, indicating that the lipids in the SS converted into water-soluble compounds,
419 such as organic acids, a fact supported by the comparatively higher TOC concentration
420 observed in the aqueous phase produced from SS (Figure 3 (a)).

421 For lower temperatures (250 °C), bio-crude seems to be most likely produced by reactions
422 between carbohydrates and proteins, such as Maillard reactions. In the case of LESS, the
423 higher protein content may compensate for the absence of lipids in the feedstock. It is
424 confirmed that Maillard reactions play a significant role in bio-crude production, which is
425 supported by the N-containing heterocycles detected by GC-MS (Fan et al., 2018; Zhang et al.,
426 2016). However, when the temperature increases to 350 °C, a larger amount of bio-crude is
427 produced from HTL of SS. This can be explained as follows: In one way, polar or
428 water-soluble fatty acids in the aqueous phase further convert or condense into crude-like
429 products. Fatty acids could undergo decarboxylation to produce alkenes or alkanes (Watanabe
430 et al., 2006), indicated by the significantly higher amounts of hydrocarbons found in the crude
431 phase, as shown in Figure 4. In another way, these fatty acids get converted into bio-crude

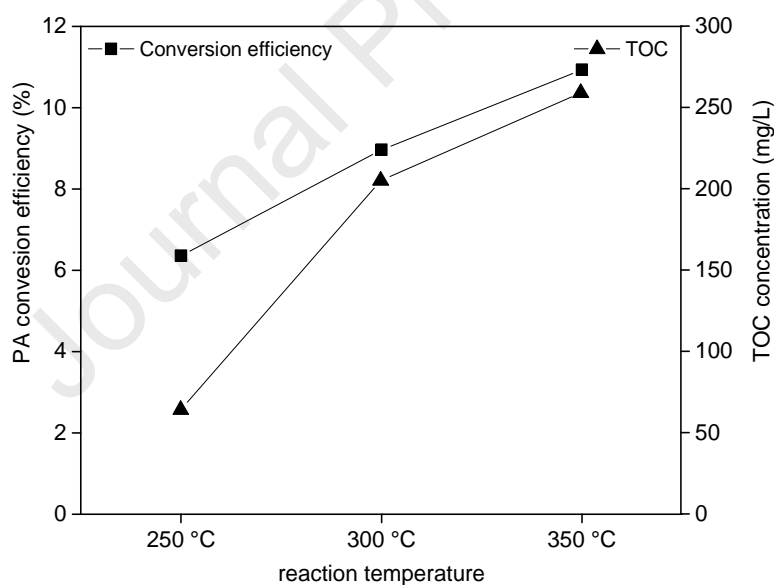
432 constituents by cross-linking reactions, like amide formation with proteins.

433 However, a fact to be taken into consideration is the limited solubility of lipids in DCM,
434 which hinders their recovery and influences the estimated values of conversion. This may
435 explain the similar yields of bio-crude reported for SS and LESS at 250 °C (Figure 2). It has
436 been reported that soap formation can happen at low temperatures in the base reaction
437 medium, which hinders product separation during the extraction of lipids from sewage
438 (Mondala et al., 2009). When the temperature increases to 350 °C, more bio-crude from HTL
439 of SS is found, which could partly be from DCM-extracted lipids.

440 **HTL of palmitic acid**

441 HTL of palmitic acid (PA) at three different temperatures was conducted to support the above-
442 made hypotheses. PA was selected as model fatty acid as it has been widely confirmed as the
443 major fatty acid in sewage sludge (Olkiewicz et al., 2014; Olkiewicz et al., 2012; Tang et al.,
444 2019; Zhu et al., 2014), also identified from FAME as shown in Figure 1. Despite the increase
445 in temperature, the carbon distribution to the solid residue was kept practically constant when
446 increasing temperature from 250 to 300 °C. Analysis of the solid residue from HTL of PA
447 (Table S3 in the Supporting Information) showed that this fraction is essentially
448 indistinguishable from palmitic acid. This fact stems from low solubility of this lipid in DCM,
449 affecting the estimation of the conversion, which presents low values when compared to HTL
450 of SS or LESS (6.4 % at 250 °C, to 10.9 % at 350 °C, Figure 5). Accordingly, the TOC
451 concentration in the aqueous phase is low, increasing from 64 to 259 mg/L, suggesting that PA
452 is resistant to decomposition below 350 °C. This is in agreement with the findings from HTL

453 of LESS and SS, where lipids only slightly contribute to the bio-crude at lower temperatures.
 454 The main portion of the unreacted PA remains solid and is collected as “solid residue”, a part
 455 of the PA is extracted by a DCM solvent to form bio-crude products. This outcome is likely
 456 due to the limited amount of DCM being unable to fully dissolve all of the fatty acids,
 457 suggesting the bio-crude yield depends on the amount of solvent and the separation procedure.
 458 This observation is greatly consistent with the reports from Watson et al.(Watson et al., 2018)
 459 and Qian et al. (Qian et al., 2017), that the extraction solvent selection should be carefully
 460 considered and normalized for the reporting of hydrothermal liquefaction yields and energy
 461 efficiency values.

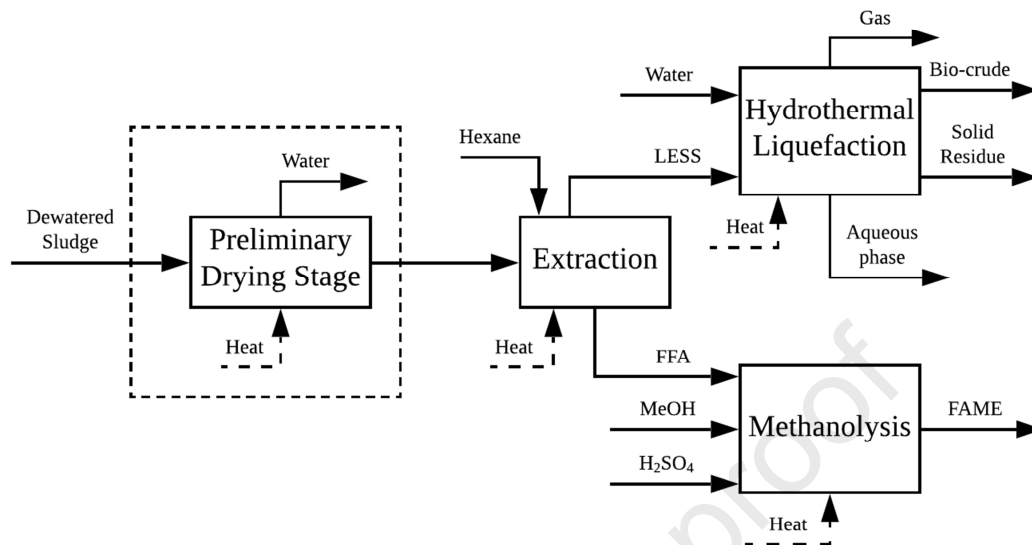


462
 463 Figure 5. Evolution of conversion and TOC concentration in the aqueous phase for HTL of PA
 464 (palmitic acid) at different temperatures.

465 4.2 Integration of lipid extraction and HTL of LESS

466 Figure 6 presents a block flow diagram of the processes considered in this work. The mass
 467 yields of the liquid fuels (bio-crude and extracted lipid) obtained in the different process

468 configurations of are shown in Table 6.



469

470 Figure 6. Block flow diagram of combined lipid extraction, HTL and methanolysis for FAME
 471 production. The checked box represents a part of the process that may be disregarded due to
 472 direct lipid extraction from wet sludge.

473 The combined yields represent the total yield of extracted lipids and bio-crude produced from
 474 LESS. Accordingly, the HHV is calculated from that of both components. When looking at
 475 the evolution of the bio-crude yield without considering lipid extraction, the jump in yield is
 476 significant between 300 °C and 350 °C, while being negligible between 250 °C and 300 °C. A
 477 similar, albeit more moderate effect can be found when performing HTL of LESS. The yield
 478 of extracted lipid exceeds the yield in bio-crude at 250 °C and 300 °C, leading to combined
 479 yields (HTL+extraction) which are more than double the value obtained using HTL alone. At
 480 350 °C, the high bio-crude yields diminish the effect of this coupling. Moreover, the
 481 calculated HHV is higher than those of the bio-crude from HTL of SS. It appears that the

482 greater efficiency of value-added fuel can be obtained from combining these two methods.
 483 Since lipids are commonly seen as biodiesel feedstock, which contains fewer heteroatoms in
 484 the target products, it is possible and efficient to extract lipids before conducting the HTL
 485 conversion in order to achieve a better energy valorization.

Table 6. Comparing the Mass yields of lipid extraction and HTL and their combination. Values in brackets correspond to the HHV of the product (MJ·kg⁻¹).

Temperature (°C)	Extraction yield (wt.%)	Liquid fuel products yields (wt.%)		
		Bio-crude of SS	Bio-crude of LESS	Combined Lipid extraction plus bio-crude
250		9.13 (32.29)	8.86 (28.85)	22.76 (35.29)
300	13.9 (39.4)	10.27 (34.60)	10.55 (34.76)	24.45 (37.39)
350		21.26 (37.26)	15.39 (34.91)	29.29 (37.04)

486 However, the higher nitrogen content in the bio-crude from HTL of LESS has to be kept in
 487 mind, as it does not meet fuel standards. Post-treatments like upgrading and distillation could
 488 be applied as effective, albeit costly, processes to reduce or remove nitrogen from bio-crude
 489 (Elliott et al., 2013; Ramirez et al., 2015). For the latter case, lesser efforts must be taken to
 490 reduce the acidity of the distillates owing to the extraction of fatty acids.

Table 7. Energy requirements (MJ·kg⁻¹) for different steps of the integrated process(without considering heat recovery).

	Combined process	HTL	Drying	Extraction	Methanolysis	Total
With drying	LESS-250 °C	45.1				221.1
	LESS-300 °C	54.9	112.8	61.0	2.2	230.9
	LESS-350 °C	64.7				240.7
Without drying	LESS-250 °C	45.1				108.3
	LESS-300 °C	54.9	-	61.0	2.2	118.1
	LESS-350 °C	64.7				127.9

491 Table 7 shows the heat requirements for the combined process. Drying is a substantial part of
 492 the energy demand, contributing to around half of the heat demand when employed. HTL and

493 lipid extraction show very similar heat demands, while the energy demand of methanolysis is
494 seemingly negligible.

495 In Table 8, estimations of energy recovery (ER, Eq. (5)), energy consumption ratio (ECR, Eq.
496 (6)) and energy demand (ED) per mass of produced bio-crude/FAME are shown. The
497 estimation has been carried out based on two cases, A and B, which employ different
498 efficiencies for combustion and heat recovery, respectively. ECR is estimated for different
499 scenarios, considering the production of only bio-crude (ECR_{BC}), both bio-crude and bio-char
500 (ECR_{BC+SR}), the former plus extracted lipid ($ECR_{BC+SR+L}$), and lipids converted into FAME
501 ($ECR_{BC+SR+FAME}$). While conventional lipid extraction requires the drying of sludge (Dufreche
502 et al., 2007; Pastore et al., 2013), recently the feasibility of performing extraction of non-dried
503 sludge (Olkiewicz et al., 2014; Pastore et al., 2013) has been shown, thus the estimations on
504 energy efficiency considers the process with and without drying step.

505 . Since the effect of temperature on the HHV of the formed phases can be neglected, the
506 energy recovery is mostly determined by the product distribution, favoring higher
507 temperatures for bio-crude formation. SS shows lower energy recovery when compared to
508 those found for LESS at the same temperature, due to the absence of the lipid phase, which
509 features a high HHV. Also, ECR values are given in Table 8. Employing only HTL in case A
510 assuming conservative efficiencies, the calculated ECR for SS is higher than 1 at temperatures
511 below 350 °C, suggesting that HTL is energetically inefficient, which aligns with the findings
512 from Xu et al. (Xu and Lancaster, 2008). However, the energy efficiency can be improved with
513 more favorable conditions, as shown for case B, and energy breakeven can always be

514 achieved. Table 8 also shows that ECR obtained for SS is lower than that obtained for LESS at
515 the same temperature, due to the energy demand for extraction and drying processes (Table 7).
516 A similar trend was reported by Vardon et al. (Vardon et al., 2012), where ECR obtained from
517 algae was lower than that from defatted algae. However, in their work, a favorable energy
518 balance was achieved (ECR 0.44 – 0.55), probably owing to the high bio-crude yields
519 (36 – 45 wt.%) and the exclusion of energy consumption for drying and lipid extraction.
520 The combined process (HTL+extraction) present higher ECRs and energy demands than the
521 case where only HTL is considered, also explainable by the additional heat requirements for
522 drying and extraction. The minimal effect of methanolysis, aided by the slightly higher HHV
523 of FAME, leads to a negligible difference in ECR between the lipid case and the FAME case
524 for all temperatures. The omission of the drying step leads to a halving of the energy demand
525 of the process. The values of the energy demand for the process with drying reported in this
526 work are lower than those obtained by Pastore et al. (Pastore et al., 2013) for the methanolysis
527 of dewatered sludge ($140 - 187 \text{ MJ} \cdot \text{kg}^{-1}_{\text{FAME}}$). However, when disregarding drying, the
528 process reaches values compared to the combined process presented by Pastore et al.
529 ($44 - 60 \text{ MJ} \cdot \text{kg}^{-1}_{\text{FAME}}$) (Pastore et al., 2013). When including the energy demand for drying,
530 this value increases greatly.

Table 8. Estimation of the Energy Recovery (ER) and Energy Consumption Ratio (ECR), as well as the Energy Demand (ED) of HTL and combined processes. Value assuming a FAME yield of 8.5 wt.% of the dry sludge.

	Process	ER	ECR _{BC}		ECR _{BC+SR}		ECR _{BC+SR+L}		ECR _{BC+SR+FAME}		Energy demand MJ/(kg BC)		Energy demand MJ/(kg FAME)	
		(%)	A	B	A	B	A	B	A	B	A	B	A	B
Only HTL	SS-250 °C	85.4	1.52	0.95	0.31	0.19	-	-	-	-	34.4	27.5	-	-
	SS-300 °C	82.1	1.54	0.96	0.78	0.48	-	-	-	-	37.2	29.7	-	-
	SS-350 °C	78.2	0.81	0.50	0.70	0.44	-	-	-	-	21.2	16.9	-	-
With drying	LESS-250 °C	98.3	1.91	1.19	0.76	0.47	1.91	1.19	1.93	1.20	185.4	147.6	110.5	88.4
	LESS-300 °C	92.3	1.69*	1.05*	0.94*	0.59*	2.02	1.26	2.03	1.26	169.7	135.1	115.4	92.4
	LESS-350 °C	96.7	1.37*	0.85*	1.06*	0.66*	2.05	1.28	2.07	1.28	121.9	97.1	120.3	96.3
Without drying	LESS-250 °C	98.3	1.91*	1.19*	0.76*	0.47*	0.93	0.58	0.94	0.59	88.9	70.4	54.1	43.3
	LESS-300 °C	92.3	1.69*	1.05*	0.94*	0.59*	1.02	0.64	1.04	0.65	85.2	67.5	59.0	47.2
	LESS-350 °C	96.7	1.37*	0.85*	1.06*	0.66*	1.08	0.67	1.10	0.68	63.7	50.5	63.9	51.1

* : only HTL of LESS is considered.

532 Conclusion

533 This work focuses on a novel proposal to maximize energy valorization of sewage sludge, by
534 integrating lipid extraction and hydrothermal liquefaction of the lipid-extracted sewage sludge
535 residue. The extracted lipid can be employed for the production of biodiesel (FAME), while
536 the remaining organics in the residual sewage sludge (lipid-extracted, LESS) can be further
537 converted into value-added products via hydrothermal liquefaction. The combined approach
538 improves the liquid bio-fuel products (29.29 wt.%) compared with HTL of un-extracted
539 sludge (21.26 wt.%) at optimized temperature. Possible key reactions during HTL have been
540 proposed based on additional experiments with model substance. The majority of lipids in the
541 sewage sludge cannot be converted into bio-crude at lower temperatures. Maillard reactions
542 significantly contribute to the formation of bio-crude components but show high nitrogen
543 contents. Regarding the energetic efficiency of the process, energy recovery of around 98 %
544 could be achieved by the coupled process, which has a significant temperature dependency.
545 Analysis of the energy consumption ratio (ECR, 1.91 – 2.05) of the process disfavors the
546 coupled process due to the energetic requirements of drying ($112.8 \text{ MJ}\cdot\text{kg}^{-1}$) and lipid
547 extraction ($61.0 \text{ MJ}\cdot\text{kg}^{-1}$). However, the energetic efficiency can be improved if making use of
548 state-of-the-art technology.

549 **Acknowledgements**

550 Armin Lautenbach, Birgit Rolli, Alexandra Böhm, Jessica Mayer, and Sonja Habicht are
551 thanked gratefully for their skillful technical assistance. Thomas Tietz and Matthias Pagel are
552 thanked for the mechanical support. Prof. Julie B. Zimmerman is greatly appreciated for all
553 valuable comments which help us to largely improve the quality of this manuscript. We would
554 like to thank the valuable comments of previous reviewers, which contributed to the quality of
555 the final work. One the authors (F.G. Fonseca) is a member of the BBW ForWerts Graduate
556 Program. The authors gratefully acknowledge the financial support from the China
557 Scholarship Council, and the National Natural Science Foundation of Anhui Province
558 (1808085QE142).

559 **References**

- 560 Biller, P., Ross, A.B., Skill, S.C., Lea-Langton, A., Balasundaram, B., Hall, C., Riley, R., Llewellyn, C.A., 2012.
 561 Nutrient recycling of aqueous phase for microalgae cultivation from the hydrothermal liquefaction process. *Algal*
 562 *Research* 1, 70-76.
- 563 Boocock, D.G.B., Konar, S.K., Leung, A., Ly, L.D., 1992. Fuels and chemicals from sewage sludge: 1. The
 564 solvent extraction and composition of a lipid from a raw sewage sludge. *Fuel* 71, 1283-1289.
- 565 Cai, M., Liu, J., Wei, Y., 2004. Enhanced Biohydrogen Production from Sewage Sludge with Alkaline
 566 Pretreatment. *Environmental Science & Technology* 38, 3195-3202.
- 567 Chen, G.Y., Hu, M.T., Du, G.Y., Tian, S., He, Z.Y., Liu, B., Ma, W.C., 2020. Hydrothermal Liquefaction of
 568 Sewage Sludge by Microwave Pretreatment. *Energy & Fuels* 34, 1145-1152.
- 569 Chopra, J., Mahesh, D., Yerrayya, A., Vinu, R., Kumar, R., Sen, R., 2019. Performance enhancement of
 570 hydrothermal liquefaction for strategic and sustainable valorization of de-oiled yeast biomass into green
 571 bio-crude. *Journal of Cleaner Production* 227, 292-301.
- 572 Demirbas, A., 2009. Combustion Efficiency Impacts of Biofuels. *Energy Sources, Part A: Recovery, Utilization,*
 573 *and Environmental Effects* 31, 602-609.
- 574 di Bitonto, L., Locaputo, V., D'Ambrosio, V., Pastore, C., 2020. Direct Lewis-Brønsted acid ethanolysis of
 575 sewage sludge for production of liquid fuels. *Applied Energy* 259, 114163.
- 576 Dote, Y., Hayashi, T., Suzuki, A., Ogi, T., 1992. Analysis of oil derived from liquefaction of sewage sludge
 577 *Fuel* 71, 1071-1073.
- 578 Dufreche, S., Hernandez, R., French, T., Sparks, D., Zappi, M., Alley, E., 2007. Extraction of Lipids from
 579 Municipal Wastewater Plant Microorganisms for Production of Biodiesel. *Journal of the American Oil Chemists'*
 580 *Society* 84, 181-187.
- 581 Elliott, D.C., Hart, T.R., Schmidt, A.J., Neuenschwander, G.G., Rotness, L.J., Olarte, M.V., Zacher, A.H.,
 582 Albrecht, K.O., Hallen, R.T., Holladay, J.E., 2013. Process development for hydrothermal liquefaction of algae
 583 feedstocks in a continuous-flow reactor. *Algal Research* 2, 445-454.
- 584 Fan, Y., Hornung, U., Dahmen, N., Kruse, A., 2018. Hydrothermal liquefaction of protein-containing biomass:
 585 study of model compounds for Maillard reactions. *Biomass Conversion and Biorefinery* 8, 909-923.
- 586 Fox, J.T., Zook, A.N., Freiss, J., Appel, B., Appel, J., Ozsuer, C., Sarac, M., 2019. Thermal conversion of
 587 blended food production waste and municipal sewage sludge to recoverable products. *Journal of Cleaner*
 588 *Production* 220, 57-64.
- 589 Frank, E.D., Elgowainy, A., Han, J., Wang, Z., 2012. Life cycle comparison of hydrothermal liquefaction and
 590 lipid extraction pathways to renewable diesel from algae. *Mitigation and Adaptation Strategies for Global*
 591 *Change* 18, 137-158.
- 592 Gao, J., Wang, Y., Yan, Y., Li, Z., Chen, M., 2020. Protein extraction from excess sludge by alkali-thermal
 593 hydrolysis. *Environ Sci Pollut Res Int* 27, 8628-8637.
- 594 Gherghel, A., Teodosiu, C., De Gisi, S., 2019. A review on wastewater sludge valorisation and its challenges in
 595 the context of circular economy. *Journal of Cleaner Production* 228, 244-263.
- 596 Huang, Y., Chen, Y., Xie, J., Liu, H., Yin, X., Wu, C., 2016. Bio-oil production from hydrothermal liquefaction
 597 of high-protein high-ash microalgae including wild Cyanobacteria sp. and cultivated Bacillariophyta sp. *Fuel* 183,
 598 9-19.
- 599 Huo, H., Wang, M., Bloyd, C., Putsche, V., 2009. Life-Cycle Assessment of Energy Use and Greenhouse Gas
 600 Emissions of Soybean-Derived Biodiesel and Renewable Fuels. *Environmental Science & Technology* 43,

- 601 750-756.
- 602 Inoue, S., Sawayama, S., Ogi, T., Yokoyama, S.-y., 1996. Organic composition of liquidized sewage sludge.
603 *Biomass and Bioenergy* 10, 37-40.
- 604 Jena, U., Vaidyanathan, N., Chinnasamy, S., Das, K.C., 2011. Evaluation of microalgae cultivation using
605 recovered aqueous co-product from thermochemical liquefaction of algal biomass. *Bioresour Technol* 102,
606 3380-3387.
- 607 Jimenez, J., Vedrenne, F., Denis, C., Mottet, A., Déléris, S., Steyer, J.-P., Cacho Rivero, J.A., 2013. A statistical
608 comparison of protein and carbohydrate characterisation methodology applied on sewage sludge samples. *Water*
609 *Research* 47, 1751-1762.
- 610 Kapusta, K., 2018. Effect of ultrasound pretreatment of municipal sewage sludge on characteristics of bio-oil
611 from hydrothermal liquefaction process. *Waste management v. 78*, pp. 183-190-2018 v.2078.
- 612 Kech, C., Galloy, A., Fripiat, C., Piel, A., Garot, D., 2018. Optimization of direct liquid-liquid extraction of
613 lipids from wet urban sewage sludge for biodiesel production. *Fuel* 212, 132-139.
- 614 Kruse, A., Dahmen, N., 2018. Hydrothermal biomass conversion: Quo vadis? *The Journal of Supercritical Fluids*
615 134, 114-123.
- 616 Kwon, E.E., Kim, S., Jeon, Y.J., Yi, H., 2012. Biodiesel Production from Sewage Sludge: New Paradigm for
617 Mining Energy from Municipal Hazardous Material. *Environmental Science & Technology* 46, 10222-10228.
- 618 Li, H., Liu, Z., Zhang, Y., Li, B., Lu, H., Duan, N., Liu, M., Zhu, Z., Si, B., 2014. Conversion efficiency and oil
619 quality of low-lipid high-protein and high-lipid low-protein microalgae via hydrothermal liquefaction.
620 *Bioresource Technology* 154, 322-329.
- 621 Liu, R., Tian, W., Kong, S., Meng, Y., Wang, H., Zhang, J., 2018. Effects of inorganic and organic acid
622 pretreatments on the hydrothermal liquefaction of municipal secondary sludge. *Energy Conversion and*
623 *Management* 174, 661-667.
- 624 Minowa, T., Kondo, T., Sudirjo, S.T., 1998. Thermochemical liquefaction of indonesian biomass residues.
625 *Biomass and Bioenergy* 14, 517-524.
- 626 Mondala, A., Liang, K., Toghiani, H., Hernandez, R., French, T., 2009. Biodiesel production by in situ
627 transesterification of municipal primary and secondary sludges. *Bioresource Technology* 100, 1203-1210.
- 628 Olkiewicz, M., Caporgno, M.P., Fortuny, A., Stüber, F., Fabregat, A., Font, J., Bengoa, C., 2014. Direct liquid-
629 liquid extraction of lipid from municipal sewage sludge for biodiesel production. *Fuel Processing Technology*
630 128, 331-338.
- 631 Olkiewicz, M., Fortuny, A., Stüber, F., Fabregat, A., Font, J., Bengoa, C., 2012. Evaluation of Different Sludges
632 from WWTP as a Potential Source for Biodiesel Production. *Procedia Engineering* 42, 634-643.
- 633 Pastore, C., Lopez, A., Lotito, V., Mascolo, G., 2013. Biodiesel from dewatered wastewater sludge: a two-step
634 process for a more advantageous production. *Chemosphere* 92, 667-673.
- 635 Peccia, J., Westerhoff, P., 2015. We Should Expect More out of Our Sewage Sludge. *Environ Sci Technol* 49,
636 8271-8276.
- 637 Pokoo-Aikins, G., Heath, A., Mentzer, R.A., Sam Mannan, M., Rogers, W.J., El-Halwagi, M.M., 2010. A
638 multi-criteria approach to screening alternatives for converting sewage sludge to biodiesel. *Journal of Loss*
639 *Prevention in the Process Industries* 23, 412-420.
- 640 Posmanik, R., Cantero, D.A., Malkani, A., Sills, D.L., Tester, J.W., 2017. Biomass conversion to bio-oil using
641 sub-critical water: Study of model compounds for food processing waste. *The Journal of Supercritical Fluids* 119,
642 26-35.
- 643 Qian, L., Wang, S., Savage, P.E., 2017. Hydrothermal liquefaction of sewage sludge under isothermal and fast

- 644 conditions. *Bioresource Technology* 232, 27-34.
- 645 Ramirez, J., Brown, R., Rainey, T., 2015. A Review of Hydrothermal Liquefaction Bio-Crude Properties and
646 Prospects for Upgrading to Transportation Fuels. *Energies* 8, 6765-6794.
- 647 Rao, U., Posmanik, R., Hatch, L.E., Tester, J.W., Walker, S.L., Barsanti, K.C., Jassby, D., 2018. Coupling
648 hydrothermal liquefaction and membrane distillation to treat anaerobic digestate from food and dairy farm waste.
649 *Bioresource Technology* 267, 408-415.
- 650 Sawayama, S., Minowa, T., Yokoyama, S.Y., 1999. Possibility of renewable energy production and CO₂
651 mitigation by thermochemical liquefaction of microalgae. *Biomass and Bioenergy* 17, 33-39.
- 652 Shahi, T., Beheshti, B., Zenouzi, A., Almasi, M., 2020. Bio-oil production from residual biomass of microalgae
653 after lipid extraction: The case of *Dunaliella* Sp. *Biocatalysis and Agricultural Biotechnology* 23, 101494.
- 654 Siddiquee, M.N., Rohani, S., 2011. Lipid extraction and biodiesel production from municipal sewage sludges: A
655 review. *Renewable and Sustainable Energy Reviews* 15, 1067-1072.
- 656 Speight, J.G., 2015. *Handbook of petroleum product analysis*. John Wiley & Sons.
- 657 Supaporn, P., Yeom, S.H., 2016. Optimization of a two-step biodiesel production process comprised of lipid
658 extraction from blended sewage sludge and subsequent lipid transesterification. *Biotechnology and Bioprocess
659 Engineering* 21, 551-560.
- 660 Suzuki, A., Nakamura, T., Yokoyama, S.-Y., Ogi, T., Koguchi, K., 1988. CONVERSION OF SEWAGE
661 SLUDGE TO HEAVY OIL BY DIRECT THERMOCHEMICAL LIQUEFACTION. *Journal of Chemical
662 Engineering of Japan* 21, 288-293.
- 663 Syed-Hassan, S.S.A., Wang, Y., Hu, S., Su, S., Xiang, J., 2017. Thermochemical processing of sewage sludge to
664 energy and fuel: Fundamentals, challenges and considerations. *Renewable and Sustainable Energy Reviews* 80,
665 888-913.
- 666 Tang, S., Shi, Z., Tang, X., Yang, X., 2019. Hydrotreatment of biocrudes derived from hydrothermal liquefaction
667 and lipid extraction of the high-lipid *Scenedesmus*. *Green Chemistry* 21, 3413-3423.
- 668 Vardon, D.R., Sharma, B.K., Blazina, G.V., Rajagopalan, K., Strathmann, T.J., 2012. Thermochemical
669 conversion of raw and defatted algal biomass via hydrothermal liquefaction and slow pyrolysis. *Bioresour
670 Technol* 109, 178-187.
- 671 Vardon, D.R., Sharma, B.K., Scott, J., Yu, G., Wang, Z., Schideman, L., Zhang, Y., Strathmann, T.J., 2011.
672 Chemical properties of biocrude oil from the hydrothermal liquefaction of *Spirulina* algae, swine manure, and
673 digested anaerobic sludge. *Bioresource Technology* 102, 8295-8303.
- 674 Wang, W., Yu, Q., Meng, H., Han, W., Li, J., Zhang, J., 2018. Catalytic liquefaction of municipal sewage sludge
675 over transition metal catalysts in ethanol-water co-solvent. *Bioresource Technology* 249, 361-367.
- 676 Watanabe, M., Iida, T., Inomata, H., 2006. Decomposition of a long chain saturated fatty acid with some
677 additives in hot compressed water. *Energy Conversion and Management* 47, 3344-3350.
- 678 Watson, J., Lu, J., de Souza, R., Si, B., Zhang, Y., Liu, Z., 2018. Effects of the extraction solvents in
679 hydrothermal liquefaction processes: Biocrude oil quality and energy conversion efficiency. *Energy*.
- 680 Xu, C., Lancaster, J., 2008. Conversion of secondary pulp/paper sludge powder to liquid oil products for energy
681 recovery by direct liquefaction in hot-compressed water. *Water Research* 42, 1571-1582.
- 682 Yang, J., He, Q., Yang, L., 2019. A review on hydrothermal co-liquefaction of biomass. *Applied Energy* 250,
683 926-945.
- 684 Zhai, Y., Chen, H., Xu, B., Xiang, B., Chen, Z., Li, C., Zeng, G., 2014. Influence of sewage sludge-based
685 activated carbon and temperature on the liquefaction of sewage sludge: Yield and composition of bio-oil,
686 immobilization and risk assessment of heavy metals. *Bioresource Technology* 159, 72-79.

- 687 Zhang, C., Tang, X., Sheng, L., Yang, X., 2016. Enhancing the performance of Co-hydrothermal liquefaction for
688 mixed algae strains by the Maillard reaction. *Green Chem.* 18, 2542-2553.
- 689 Zhu, F., Zhao, L., Jiang, H., Zhang, Z., Xiong, Y., Qi, J., Wang, J., 2014. Comparison of the Lipid Content and
690 Biodiesel Production from Municipal Sludge Using Three Extraction Methods. *Energy & Fuels* 28, 5277-5283.
- 691

Journal Pre-proof

Highlights

- Raw sewage sludge was submitted to lipid extraction.
- Raw and lipid-extracted sewage sludge, and a model lipid were subjected to HTL.
- Combined process (HTL+extraction) yielded 29.3 wt.% liquid fuel-like products.
- Combined process showed an energy recovery up to 98 % based on HHV comparison.
- Energy consumption ratio shows a significant temperature dependency.

Declaration of interests

The authors declare that they have no known competing financial interests or personal relationships that could have appeared to influence the work reported in this paper.

Journal Pre-proof